Author Manuscript

Author Manuscript

Author Manuscript

Author Manuscript

HHS Public Access

Author manuscript

Cancer Res. Author manuscript; available in PMC 2016 April 01.

Published in final edited form as:

Cancer Res. 2015 April 1; 75(7): 1399–1412. doi:10.1158/0008-5472.CAN-14-2785.

PDK1 and SGK3 contribute to the growth of BRAF mutant melanomas and are potential therapeutic targets

Marzia Scortegagna[1], **Eric Lau**, **Tongwu Zhang**[2], **Yongmei Feng**[1], **Chris Sereduk**[3], **Hongwei Yin**[3], **Surya K. De**[1], **Katrina Meeth**[4], **James T. Platt**[4], **Casey G. Langdon**[4], **Ruth Halaban**[4], **Maurizio Pellecchia**[1], **Michael A. Davies**[5], **Kevin Brown**[2], **David F. Stern**[4], **Marcus Bosenberg**[4], and **Ze'ev A. Ronai**

[1]Cancer Center, Sanford-Burnham Medical Research Institute, La Jolla, CA

[2]Division of Cancer Epidemiology & Genetics, Laboratory of Translational Genomics, NCI, Bethesda, DC

[3]Cancer and Cell Biology Division, The Translational Genomics Research Institute (TGen), Phoenix, Arizona

[4]Departments of Dermatology and Pathology, Yale University, School of Medicine, New Haven, CT

[5]Melanoma Medical Oncology, MD Anderson Cancer Center, Houston, TX

Abstract

Melanoma development involves members of the AGC kinase family including AKT, PKC and, most recently, PDK1, as elucidated recently in studies of *Braf::Pten* mutant melanomas. Here we report that PDK1 contributes functionally to skin pigmentation and to the development of melanomas harboring a wild-type PTEN genotype, which occurs in ~70% of human melanomas. The PDK1 substrate SGK3 was determined to be is an important mediator of PDK1 activities in melanoma cells. Genetic or pharmacological inhibition of PDK1 and SGK3 attenuated melanoma growth by inducing G1 phase cell cycle arrest. In a synthetic lethal screen, pan-PI3K inhibition synergized with PDK1 inhibition to suppress melanoma growth, suggesting that focused blockade of PDK1/PI3K signaling might offer a new therapeutic modality for wild-type PTEN tumors. We also noted that responsiveness to PDK1 inhibition associated with decreased expression of pigmentation genes and increased expression of cytokines and inflammatory genes, suggesting a method to stratify melanoma patients for PDK1-based therapies. Overall, our work highlights the potential significance of PDK1 as a therapeutic target to improve melanoma treatment.

Keywords

PDK1; SGK; BRAF; PTEN; melanoma; Cyclin D1; MITF

Correspondence to: Ze'ev Ronai, Sanford-Burnham Medical Research Institute, 10901 N. Torrey Pines Rd, La Jolla, CA, 92037. ronai@sbmri.org.

Disclosure of Potential Conflicts of Interest. There are no potential conflicts of interest to disclose by all authors.

Author Manuscript Author Manuscript Author Manuscript Author Manuscript

INTRODUCTION

Approximately 70% of melanomas with mutated BRAF also exhibit the inactivation of the tumor suppressor PTEN, resulting in constitutive activation of the phosphoinositide 3-kinase (PI3K) signaling pathway (1). Phosphoinositide-dependent kinase 1 (PDK1), an immediate downstream effector of PI3K, is a master kinase able to phosphorylate more than 20 members of the AGC kinase family, which includes PKA, AKT, PKC, p70S6k, and SGK (2,3). The relationship between PDK1 and PTEN was first revealed by the demonstration that the lethality of PTEN deficiency in flies was rescued by deletion of PDK1, establishing PDK1 as the main downstream effector of PI3K (4). Recently, we investigated the role of PDK1 in melanomas using a mouse model in which expression of mutated *BRAF* (*BRAF*^{V600E}) and deletion of *Pten* is conditionally and specifically activated in melanocytes (5). Using this model, we showed that genetic inactivation or pharmacological inhibition of PDK1 delays melanoma development and metastasis. However, wild-type (WT) *PTEN* is expressed in a sizable fraction (~70%) of BRAF mutant human melanomas (1,6,7), and the role of PDK1 in the progression of such melanomas is unknown. Here, we used genetic and pharmacological models to show that PDK1 plays an even more significant role in the development of WT *PTEN*, *BRAF*^{V600E} mouse and human melanomas, compared with the *PTEN*-deficient, *BRAF*^{V600E} melanomas.

Although studies in several cancer types suggest that AKT is the main downstream effector of the PI3K/PDK1 signaling pathway, increasing evidence indicates that additional factors are equally important (8–10). For example, the overexpression of AKT in PDK1 knockout (KO) cancer cells was demonstrated to be insufficient to restore the malignant phenotype (11).

The three isoforms of the SGK family of AGC kinases, SGK1, SGK2, and SGK3, are also activated by the PI3K/PDK1 signaling pathway. SGKs exhibit similar substrate specificity to AKT, and both kinases influence the activity of proteins involved in cell growth, survival, and migration (12,13). Several studies have demonstrated important roles for the SGK isoforms in PI3K signaling in both physiological and pathological conditions. SGK1 and SGK3 are ubiquitously expressed, whereas SGK2 is restricted to the kidney, pancreas, liver, and brain. Given the function of SGK1 and SGK3 in cell proliferation and survival, it is not surprising that they have been shown to be involved in the growth of several cancers (14,15). However, their contribution in melanoma remains unclear.

In this study, we identify SGKs as key mediators of PDK1 activity in melanoma and demonstrate the importance of the PDK1/SGK signaling axis in the growth of PTEN WT melanomas. We also demonstrate that PI3K inhibitor can synergize with PDK1 inhibitors in suppressing melanoma growth, and point to possible means for the stratification of human *BRAF*^{V600E} *PTEN* WT tumors for PDK-targeted therapies.

Author Manuscript Author Manuscript Author Manuscript Author Manuscript

MATERIALS AND METHODS

Primary melanoma cells and human melanoma cell lines

Murine melanoma cells Sanford Burnham Melanoma A2 (SBM-A2) and SBM-A3 were derived from primary cutaneous lesions from *Braf*^{V600E}*::Pten*$^{+/+}$*::Cdkn2a*$^{-/-}$ mice. Tumors were cut in small parts and digested with collagenase (10 mg/ml; Sigma) for 1 h at 37°C and filtered through a 100-μm nylon cell strainer (BD Falcon). Cells were resuspended in DMEM supplemented with 10% fetal bovine serum (FBS) and penicillin/streptomycin, and incubated at 37°C. Once established, cell lines were passaged twice before use in experiments. The mouse YUMM1.5 and YUMM1.9 and the human 501MEL and UACC903 cell lines were maintained in DMEM medium supplemented with 10% FBS and penicillin/streptomycin. Low passage human melanoma cells YUHEF, YUSIK, YUMAC, YUGASP, AND YUROB were obtained from the Tissue Resource Core of the Yale SPORE in Skin Cancer and all cell lines were used at or under passage 25 as has been described (16). These melanoma cells were maintained in OptiMEM supplemented with 5% FBS and 1%penicillin/streptomycin. Information on the genotype and origin of the cell lines used is shown in Supplementary Table 2.

Activation of the *Tyr::CreER*^{T2} transgene

4-Hydroxytamoxifen (4-HT) was prepared at 50 mg/ml in DMSO and 10 μl was applied to the dorsal skin on postnatal days 1, 3, and 5 using a small paintbrush.

Histological analyses

Tumors sections were fixed overnight in Z-Fix (buffered zinc formalin fixative, Anatech) at 4°C. Sections were then washed twice with PBS and processed for paraffin embedding. Paraffin blocks were sliced at 5 μm and sections were stained with hematoxylin and eosin (H&E).

Antibodies and reagents

The following antibodies were purchased from Cell Signaling Technologies: pNDRG1, pPDK1, pAKT308, pAKT473, pGSK3β (Ser 9), pPRAS40 (Thr 246), pFOXO3a (Thr 32), pERK1/2, AKT, FOXO3a, pP70S6K (Thr 389), pS6K (Ser 235/236), PRAS40, GSK3b, ERK1/2, SGK3, cyclin D1, PTEN, P70S6K, and S6. Antibodies against β-actin, SGK1, PKC, and tubulin were purchased from Santa Cruz Biotechnology. 4-Hydroxytamoxifen and antibodies against S100 were purchased from Sigma. Synthesis of the PDK1 inhibitor GSK2334470 was performed as previously described (5).

Gene silencing and transfection

shRNA for mouse *Pdk1*, *Sgk1*, and *Sgk3* were purchased from Sigma. Viral particles were produced in HEK293T cells transfected with the plasmid of interest and appropriated packaging plasmids using Jet Prime (Polyplus transfection). Target cells were infected with viral particles by spinoculation in the presence of polybrene (4 μg/ml, Sigma). Stable clones were established by growth in media containing puromycin (1 μg/ml, InVivoGen).

Author Manuscript Author Manuscript Author Manuscript Author Manuscript

Western blotting

Cells were harvested and lysed in RIPA buffer (50 mM Tris-HCl, pH 7.5, 150 mM NaCl, 1% Triton X-100, 0.1% SDS, 0.1% sodium deoxycholate, 1 mM EDTA, 1 mM sodium orthovanadate, 1 mM PMSF, 10 μg/ml aprotinin, and 10 μg/ml leupeptin). Cell lysates were subjected to SDS-PAGE and the proteins were transferred onto nitrocellulose membranes (Osmonics Inc.). Membranes were incubated with primary antibodies for 18 h at 4°C, washed, and then incubated with secondary antibody conjugated with fluorescent dye. After processing, membranes were analyzed using the Odyssey Imaging System (Amersham Biosciences).

Immunofluorescence microscopy

Sections of skin and lymph nodes prepared as described above were deparaffinized, rehydrated, washed in PBS, and incubated with Dako Protein Block for 30 min at room temperature. Antigen retrieval for S100 immunostaining was performed by incubation in citrate buffer (pH 6.0) in a decloaking chamber (Biocare Medical). Antibodies were diluted in Dako antibody diluent at 1:500 and incubated with sections overnight at 4°C. Secondary antibodies conjugated to Alexa Fluor 594 (Molecular Probes) were diluted to 1: 400 and incubated with sections for 1 h at room temperature. Nuclei were counterstained with SlowFade Gold anti-fade reagent containing 4′,6-diamidino-2-phenylindole (DAPI; Vector).

qRT-PCR analysis

Total RNA was extracted using a miniprep kit (Sigma) and digested with DNase I. cDNA was synthesized using oligo-dT and random hexamer primers and QPCR was performed on biological triplicates using SYBR Green. Amplification of histone H3.3A served as an internal control. The PCR primers were designed using Primer3 and their specificity was checked using BLAST. The PCR products were limited to 100–200 base pairs. Primer sequences were: mouse *H3.3a*: forward, 5′-aagcagactgcccgcaaat-3′ and reverse, 5′-ggcctgtaacgatgaggtttc-3′; mouse *Pdk1*: forward, 5′-acgccctgaagacttcaagtttg-3′ and reverse, 5′-gccagttctcgggccaga-3′; mouse *Sgk1*: forward, 5′-cgtccgaacgggacaacat-3′ and reverse, 5′-gtccaccgtccggtcatac-3′; mouse *Sgk3*: forward, 5′-tcccagctctgacgaacaca-3′ and reverse, 5′-tcaaactctgcgtatctcctga-3′; mouse *Dct*: forward, 5′-gtcctccactcttttacagacg-3′ and reverse, 5′-attcggttgtgaccaatgggt-3′; mouse *Tyr*: forward, 5′-tctggacctcagttccccttc-3′ and reverse, 5′-aacttacagtttccgcagttga-3′; mouse *Il6*: forward, 5′-ctgcaagagacttccatccag-3′ and reverse, 5′-agtggtatagacaggtctgttgg-3; mouse *Mmp3*: forward, 5′-ggcctggaacagtcttggc-3′ and reverse, 5′-tgtccatcgttcatcatcgtca-3′; mouse *Zeb1*: forward, 5′-accgccgtcatttatcctgag-3′ and reverse, 5′-catctggtgttccgttttcatca-3′.

Quantification of lymph node metastasis

Immunofluorescent staining of S100 in lymph node sections was performed as described above. S100-positive tumor cells in the sections were quantified by first scanning at 20× magnification with the Aperio ScanScope FL system (Aperio Technologies) and then analyzing cell numbers using the Area Quantification FL algorithm (version 11, Aperio Technologies). The algorithm was tuned using a preset procedure and the subsequent macro was saved and applied to all slides.

Author Manuscript Author Manuscript Author Manuscript Author Manuscript

Colony formation assay

Five hundred tumor cells were plated into each well of a 6-well plate and incubated for 7-to-12 days. Viable colonies were stained with crystal violet (Sigma-Aldrich) and the plates were imaged. The colony numbers and intensity were determined using ImageJ software. Each experiment was performed at least three times.

Animal studies and in vivo experiments

All mouse experiments were performed under the guidelines of the Institutional Animal Care and Use Committee (IACUC) of Sanford-Burnham Medical Research Institute. *Braf*^{V600E}*::Cdkn2a*$^{-/-}$*::Pten*$^{+/+}$ and *Pdk1*$^{-/-}$ mice were generated as previously described (17,18). Cohorts of at least six animals per group were used in each of the experimental group.

Three-dimensional growth assay

Cells were induced to form spheroids using the hanging drop method. The cells were plated at 200 cells / 20 μl/well in a Nunc-60 well microwell MiniTray. The trays were covered, inverted, and incubated at 37°C in a humidified 5% CO_2 incubator for 5 days. Spheroids from wells containing single spheroids were transferred to a 48-well plate coated with 1% low melting point agarose. Compounds or DMSO vehicle were added, and images of spheroids were captured every 48 h for 8 days using an Olympus IX-71 microscope equipped with a camera. The relative spheroid areas were measured using ImageJ64 software.

Flow cytometric cell cycle analysis

Cell lines were seeded in 6-well tissue culture plates at 1 X 10^5 cells/well, incubated overnight, and then treated with shRNAs. Cells were harvested by trypsinization, fixed in 70% ethanol in PBS at −20°C, and then stored until further use. For analysis, cells were washed once in PBS and incubated in cell cycle staining buffer (60 μg/ml propidium iodide and 0.15 mg/ml RNase A; Sigma) for 20 min. Biological triplicates of 10,000 cells (within the G1–G2 gates) per sample were collected for each experiment, and the data were analyzed using FlowJo software (TreeStar).

RPPA analysis

The cells were washed twice in ice-cold PBS, then lysed in 30 μL of RPPA lysis buffer [1% Triton X-100, 50 nmol/L Hepes (pH 7.4), 150 nmol/L NaCl, 1.5 nmol/L $MgCl_2$, 1 mmol/L EGTA, 100 nmol/L NaF, 10 nmol/L NaPPi, 10% glycerol, 1 nmol/L phenylmethylsulfonyl fluoride, 1 nmol/L Na_3VO_4, and aprotinin 10 μg/mL. Lysates were transferred at volumes of 25 to 30 μL into a PCR 96-well plate. Ten microliters of 4× SDS/2-ME sample buffer (35% glycerol, 8% SDS, 0.25 mol/L Tris-HCl, pH 6.8; with 10% β-mercaptoethanol added before use) was added to each sample well. The plates were covered and incubated for 5 minutes at 95°C and then centrifuged for 1 minute at 2,000 rpm. Samples were applied to RPPA slides as previously described (19).

Author Manuscript Author Manuscript Author Manuscript Author Manuscript

Synthetic lethal screen for PDK1 inhibitor combination

Interactions between PDKi (GSK2334470) and 45 other agents were determined in a "one versus many" screen at the Yale Center for Molecular Discovery. A master 384-well plate was set up manually, incorporating four or eight dilutions of 45 test agents to yield a range from 10 μM to 1 nM final in the experiments. The master plates also included multiple negative control wells (0.2% DMSO vehicle) and staurosporine positive "kill" controls for a final 10 μM staurosporine. The test agents consisted of 2,4-Dinitrophenol, 4u8c, 17-DMAG, 4485, atorvastatin, AZD-2014, AZD-6244, BI-D1870, BKM-120, Bortezomib, Brefeldin A, carfilzomib, cerulenin, EMD638683, EX 527, FASN211, fatostatin A, FCCP, GGTI-298, GSK650394A, GSK690693, GSK2334470, GSK2606416, Homoharringtonine, Metformin, oligomycin, PF429242, Phenformin, piperlongumine, Rosiglitazone, SB 204990, SBRI108610, SBRI108634, SBRI108684, SBRI108692, SBRI108734, SBRI108740, Simvastatin, SRT1720, STA-4783, STF-083010, T0070907, Trametinib, tunicamycin, and vemurafenib. 750–1000 cells/16 μl medium per well were dispensed into 384-well plates using a Thermo multidrop dispenser. After incubation overnight to allow cell attachment, a pin tool was used to transfer 20 nl of compounds from each well of the master plate into the 384-well test plates containing cells. Next, 4 μL of either 0.1% DMSO, or GSK233470 to yield final 2 μM or 10 μM were added. Cells were incubated an additional three days, and growth was quantified by CellTiterGlo (Promega) to read out ATP accumulation, which correlates well with viable cell number. Additivity and superadditivity were calculated using the Bliss independence model and area under the curve (AUC) calculations. To avoid over-weighting the high concentration points, the natural log concentrations are used to calculate AUC. AUC calculation is performed using the function "auc" from the R library "MESS", using the linear type option. This function approximates the area under a set of points by summing the trapezoidal segments between adjacent points. Normalization of the AUC calculation is performed by dividing the calculated AUC by the width of the log-concentration range for each plated agent to correct for differences in concentration ranges.

Statistical analysis

All data except survival curves were analyzed by the unpaired t-test. Kaplan-Meyer survival curves were compiled using Prism software (GraphPad) and statistical significance was assessed using the log-rank (Mantel-Cox) test. $P < 0.05$ was considered statistically significant.

RESULTS

PDK1 deletion promotes tumor suppression and reduces the pigmentation of $Braf^{V600E}$::$Cdkn2a^{-/-}$ mice harboring WT Pten

Our previous studies demonstrated that the genetic inactivation of PDK1 in *Braf*^{V600E}*::Cdkn2a*$^{-/-}$*::Pten*$^{-/-}$ animals significantly delays melanoma development and effectively inhibits metastasis (5). Because about 70% of human melanomas harbor WT *PTEN*, we sought to determine the effects of *Pdk1* deletion on the development and progression of melanoma in *Braf*^{V600E}*::Cdkn2a*$^{-/-}$*::Pten*$^{+/+}$ mice. In these mice, the expression of *Braf*^{V600E} is induced specifically in melanocytes by the administration of the estrogen analog 4-hydroxytamoxifen (4-HT) (5). *Braf*^{V600E}*::Cdkn2a*$^{-/-}$*::Pdk1*$^{-/-}$ (PDK1

Author Manuscript Author Manuscript Author Manuscript Author Manuscript

KO) mice systemically treated with 4-HT on postnatal days 1, 3, and 5 exhibited markedly reduced pigmentation on day 21 after 4-HT administration compared to similarly treated *Braf*^{V600E}*::Cdkn2a*$^{-/-}$*::Pdk1*$^{+/+}$ (PDK1 WT) mice (Fig. 1A, 1B). Consistent with these observations, heavy pigmentation and melanomagenesis was observed in the skin (Fig. 1C) and lymph nodes (Fig. 1D) of PDK1 WT mice, whereas it was significantly reduced in the PDK1 KO mice. Examination of mice on day 38 after 4-HT administration revealed that 7/12 (40%) PDK1 WT mice contained tumors, whereas tumors were undetectable in the PDK1 KO mice (Fig. 1E). Moreover, the mean survival time of the PDK1 KO mice was significantly prolonged compared with that of the PDK1 WT mice (76 vs. 42 days; $P < 0.001$; Fig. 1F). Notably, only a single administration of 4-HT was required to observe the effects of PDK1 deletion on melanomagenesis in the *Braf*^{V600E}*::Cdkn2a*$^{-/-}$ animals (Supplementary Fig. S1A). Under these conditions, tumor development was delayed (≥ 50 days) but still markedly reduced in the PDK1 KO (2/8 mice) compared with the PDK1 WT (12/14 mice) mice (Supplementary Fig. S1).

The marked effects of PDK1 deletion on melanomagenesis in *Braf*^{V600E}*::Cdkn2a*$^{-/-}$ were confirmed by immunohistochemical and immunofluorescent evaluation of the skin. Consistent with these effects, we observed the presence of significantly reduced pigmented, hyperproliferative foci within the skin sections (Fig. 1G) and lymph nodes (Fig. 1I) from PDK1 KO compared with PDK1 WT mice. Similarly, immunofluorescence staining for S100, a marker for both melanotic and amelanotic melanomas, revealed substantially more tumor cells within the skin (Fig. 1H) and more extensive invasion of the lymph nodes (Fig. 1J) of PDK1 WT compared with PDK KO mice.

We next investigated some of the key signal transduction pathways regulated by PDK1. For this, we established early (1–2)-passage cell cultures of tumors from *Braf*^{V600E}*::Cdkn2a*$^{-/-}$*::Pten*$^{+/+}$*::Pdk1*$^{-/-}$ and *Braf*^{V600E}*::Cdkn2a*$^{-/-}$*::Pten*$^{+/+}$*::Pdk1*$^{+/+}$ mice, which enabled the analysis of AGC kinase pathway components. As expected, the absence of PDK1 resulted in a marked reduction in the phosphorylation of downstream target proteins such as AKT, FOXO3a, GSK3β, PRAS40, RSK, p70S6K, and the SGK1 substrate NDRG1 (Fig. 1K).

Collectively, these data establish that PDK1 plays an important role in the development of melanoma in *Braf*^{V600E}*/WT Pten* mice, in addition to its reported role in the *Braf*^{V600E} mice in which *Pten* is inactivated or deleted.

SGK1 and SGK3 are key mediators of PDK1-dependent melanomagenesis

The results shown above identify several potential PDK1 substrates that might be required for melanoma development in *Pdk1* WT mice, including the transcription factor FOXO3a, which was also identified in our earlier study (5). Notably, FOXO3a is regulated by phosphorylation of the same phosphoacceptor sites by either AKT or SGK. To determine whether SGK1 or SGK3 play a role in PDK1-dependent melanoma development, we performed shRNA-mediated knockdown (KD) of *Pdk1*, *Sgk1*, or *Sgk3* in two melanoma lines each derived from *Braf*^{V600E}*::Cdkn2a*$^{-/-}$*::Pten*$^{-/-}$ mice (lines YUMM1.5 and YUMM1.9) and *Braf*^{V600E}*::Cdkn2a*$^{-/-}$*::Pten*$^{+/+}$ mice (lines SBM-A2 and SBM-A3) and examined the effects of KD on the expression and phosphorylation of key PDK1 signaling

Author Manuscript Author Manuscript Author Manuscript Author Manuscript

components (Fig. 2A and Supplementary Fig. S2A–D). As expected, the degree of AKT, FOXO3a and PRAS40 phosphorylation was notably lower in the PTEN WT tumor cells, reflecting PTEN activity (Fig. 2A). The degree of the KD for *Pdk1*, *Sgk1* and *Sgk3* was largely efficient (Supplementary Fig. S2A–D). PDK1 KD effectively attenuated phosphorylation of FOXO3a, NDRG1, S6, P70S6K, and 4EBP1 in both *Pten* WT and mutant cell lines (Fig. 2B and Supplementary Fig. S2E). In contrast, KD of *Sgk1* abolished phosphorylation of NDRG1 but had minimal effects on p70S6K, FOXO3a, PRAS40 and 4EBP1, and KD of *Sgk3* reduced phosphorylation of 4EBP1, P70S6K, and S6 but had no effect on NDRG1 (Fig. 2B and Supplementary Fig. S2E). Consistent with recent reports that SGK3 and p70S6K regulate cyclin D1 expression and cell growth (20), we observed reduced cyclin D1 expression after KD of PDK1 and SGK3, but not KD of SGK1 (Fig. 2B and Supplementary Fig. S2E). The effects of SGK3 KD on p70S6K phosphorylation and cyclin D1 protein expression in melanoma cells were confirmed using an independent *Sgk3*-specfic shRNA (Supplementary Fig. S2G). These results demonstrate that the effects of PDK1 inhibition are closely mimicked by SGK3 inhibition, raising the possibility that this protein might mediate the effects of PDK1 on growth of mutant *Braf*, *Pten* WT melanomas.

To test this further, we examined colony formation and three-dimensional growth of YUMM1.5 ($Pten^{-/-}$) and SBM-A2 ($Pten^{+/+}$) cell lines expressing control or *Pdk1*-, *Sgk1*-, and *Sgk3*-targeted shRNA. We found that clonal growth was virtually abolished by KD of *Pdk1* or *Sgk3* but minimally affected by *Sgk1* KD (Fig. 2C, Fig. 2D). Notably, KD of all three proteins reduced melanoma sphere formation and growth to some extent, with *Pdk1* KD the most effective (90% inhibition versus cells expressing scrambled shRNA), followed by *Sgk3* KD (70% inhibition) and *Sgk1* KD (55% inhibition; Fig. 2E). These effects were confirmed using independent *Sgk1*- or *Sgk3*-targeted shRNAs (~50% inhibition of sphere formation over 7 days; Supplementary Fig. S2F, S2H, S2I). These data demonstrate that SGK3 inhibition effectively inhibits colony formation and 3D growth of $BRAF^{V600E}$ *PTEN* WT and PTEN null melanomas.

Pharmacological inhibition of SGK3 inhibits melanoma cell growth

We next asked whether pharmacological inhibition of PDK1 and SGK would phenocopy the genetic inactivation with shRNA. To this end, we treated the $Braf^{V600E}::Cdkn2a^{-/-}::Pten^{-/-}$ and $Braf^{V600E}::Cdkn2a^{-/-}::Pten^{+/+}$ cell cultures with either the SGK inhibitor (SGKi) GSK650394 (21) or the PDK1 inhibitor (PDK1i) GSK2334470 (22) for 24 h and then examined PDK1-dependent signaling pathway components. Confirming the expected effects, PDK1i reduced the phosphorylation of all of its downstream components, whereas SGKi reduced NDRG1 and S6 phosphorylation, but did not affect the upstream components FOXO3a and PRAS40 (Fig. 3A). We next examined the effects of pharmacological SGKi on sphere formation of YUMM1.5 cells incubated with the PDK1i and SGKi. Both inhibitors were effective and essentially abolished sphere formation at high concentrations, whereas the effect of PDK1i was more pronounced at lower concentrations (Fig. 3B–C). These results suggest that the role of PDK1 in melanoma growth is mediated, at least in part, by SGK.

Author Manuscript Author Manuscript Author Manuscript Author Manuscript

Inhibition of SGK3 or PDK1 causes melanoma cell cycle arrest at G1

To determine the mechanism(s) by which genetic or pharmacological inhibition of SGK3 suppresses melanoma growth, we performed FACS analysis to determine the proportion of cells in each phase of the cell cycle after KD of PDK1 or SGK3. We found that the expression of either *shSgk3* or *shPdk1* led to the accumulation of $Braf^{V600E}::Cdkn2a^{-/-}::Pten^{-/-}$ and $Braf^{V600E}::Cdkn2a^{-/-}::Pten^{+/+}$ cells in G1 (Fig. 4), and this finding was confirmed using an independent *Sgk3*-specific shRNA (Supplementary Fig. S3). These results indicate that the observed changes in cell growth following the inhibition of SGK3 and PDK1 activity are attributed to cell cycle arrest at the G1 phase.

PDK1 inhibition synergizes with proteasome and PI3K/mTOR inhibition to attenuate melanoma growth

Combination therapies are often more potent inhibitors of tumor growth and can also suppress the growth of tumors resistant to the individual therapies. Therefore, we next screened for pharmacological inhibitors that might act synergistically with PDK1i in suppressing melanoma growth. For this, we tested the PDK1 inhibitor (GSK2334470) in combination with 45 known inhibitors, including modulators of MAPK and PI3K activity, ER stress, metabolic stress, and of reactive oxygen species (Fig. 5A). To ensure coverage of multiple subtypes, we tested melanoma lines including *BRAF* mutant, *HRAS* mutant, *NRAS* mutant and WT for *BRAF*, *HRAS* and *NRAS*. Cell growth was analyzed after treatment with 2 μM or 10 μM of the PDK1 inhibitor over a broad range of doses of the second agent (Supplementary Fig. S4). Determination of synergy was made by monitoring inhibition of combination therapy minus Bliss additivity of individual agent responses. This assessment revealed that 50% greater effect was identified compared with what would have been predicted by additivity in 24 conditions.

Among the compounds showing potent synergistic activity with GSK2334470 in suppressing growth were the pan PI3K inhibitor BKM120 and the proteasome inhibitors bortezomib and carfilzomib (Fig. 5A and Supplementary Fig. S4). In agreement with the effects on cell growth, we found that the addition of 1 or 4 nM bortezomib further inhibited phosphorylation of key PDK1 substrates compared with inhibition of PDK1 alone (AKT, FOXO3a, and S6 phosphorylation compared with PDK1 inhibition alone (Fig. 5B) and concomitantly further activated ER stress (ATF4 and CHOP induction) and apoptosis (cleaved caspase 3 and PARP; Fig 5B). A similar synergistic effect of the PDK1i and bortezomib was observed with the human melanoma cell lines UACC903 and Mel501, although the degree of caspase 3 cleavage was not detectable in the UACC903 cells, possibly due to the higher level of AKT in these cells (Fig. 5B). Notably, the synergistic effect on apoptosis of YUMM1.5 cells following co-treatment of bortezomib and PDK1 inhibitors was seen in 3D cultures only when higher concentrations of bortezomib were administered (200 nM in 3D cultures, compared with 4 nM in the 2D cultures; Fig. 5C). The latter might be attributed to the higher expression of anti-apoptotic genes in cells grown in 3D cultures, as previously reported for lung cancer cells and mesothelioma cell lines (23,24).

Author Manuscript Author Manuscript Author Manuscript Author Manuscript

The pan PI3K inhibitor BKM120 (25,26) was also found to synergize with the PDK1i in reducing AKT, FOXO3a, PRAS40 and GSK3β phosphorylation in both the PTEN WT and mutant melanoma cells (Fig. 6A). Notably, the combination of BKM120 with PDK1i induced cell death in the PTEN WT but not in the PTEN mutant melanoma cells, measured by leaved Caspase 3 levels (Fig. 6A). Nevertheless, the combination of BKM120 and PDK1i attenuated cell growth in the PTEN mutant melanoma cells, as reflected by the reduced expression of cyclin D1 (Fig. 6A). These observations indicated that the response of melanoma cells to combined inhibition of PI3K/PDK1 depends on the degree of PTEN/AKT signaling, and determines the susceptibility to undergo cytostatic or cytotoxic response.

We have further assessed the effect of the PDKi and BKM120 combination on human melanoma harboring PTEN WT or mutant genotypes. Consistent with the finding in the mouse melanoma lines, this combination was effective in inhibiting the key AKT/PDK1 signaling in both melanoma lines, albeit with greater effectiveness on the PTEN WT derived cells. Cell death program, monitored by caspase 3 cleavage, was induced in the PTEN WT (SBM-A2 and Mel501) but not PTEN mutant (YUMM1.5 and UACC903) melanomas by the BKM120 and PDK1i inhibitor combination (Fig. 6B). When assessed in 3D growth this combination elicited cytostatic effect, limiting, albeit significantly, the growth of these tumors cells (Fig. 6C).

The combined effect of PDK1 and PI3K inhibitors on the human melanoma cell lines UACC903 was analyzed by reverse phase protein arrays (RPPA) using a panel of 172 antibodies directed to components of major signaling pathways (19,27). This analysis revealed that combined PDK1 and PI3K inhibition elicited additive effect which was reflected in the degree of decreased phosphorylation of key components along the PDK1 pathway, including S6, AKT, p70S6K, as well as tuberin, mTOR and GSK3β, pointing to effect of this combination also on mTOR and GSK3 pathways (Supplementary Table S1, Fig. 5A and Supplementary Fig. S5).

These findings points for the effectiveness of combined PI3K/PDK1 inhibition, which attenuates the growth of melanoma cells, with a notably greater effect on the PTEN WT cultures.

Stratification of melanoma to PDK1 inhibition

To determine whether sensitivity of melanoma to PDK1i is associated with a specific gene signature, we assessed the effects of PDK1i on 19 melanoma cell lines for which gene expression and genomic mutation data are available. The PDK1i 50% inhibitory concentration (IC50) for cell growth and 50% effective concentration (EC50) were used to segregate the cell lines (Fig. 7A). The 7 most resistant (UACC1940, 2994, 2512, 1120, 1118, 558, and 2641) and the 7 most sensitive (UACC903, 2331, 612, 2496, 647, 952, and 3337) cell lines were then selected for ingenuity pathway analysis (IPA) to identify the genes and pathways most significantly affected by PDK1i ($P < 0.05$). This analysis identified 1,178 differentially expressed genes, including multiple components of the TIF2 nuclear co-regulator and mTOR signaling pathways that were specifically associated with sensitivity to PDK1i. Further refinement of this assessment to include only genes showing ≥ 10-fold differential expression clearly distinguished two clusters of genes associated with

Author Manuscript Author Manuscript Author Manuscript Author Manuscript

sensitivity and resistance to PDK1i (Fig. 7B). Sensitivity to PDK1i was associated with the reduced expression of several pigmentation genes (*DCT, PMEL, MelanA*) and elevation of number of cytokines and immune modulators, including *IL8, IL1B, IL6, Serpin1, Serpin2, and PDGF* (Fig. 7B). These findings were confirmed by qPCR. PDK1i-treated YUMM1.5 cells showed a reduction in *DCT* and *TYR* mRNA and an increase in *IL6* mRNA compared with untreated cells (Fig. 7C). Consistent with these results, canonical pathway analysis showed that sensitivity of melanoma cells to PDK1i was associated with decreased expression of MITF, the key upstream regulator of pigmentation genes ($P = 1.6^{E-18}$). Integrin signaling genes were also strongly associated with PDK1i sensitivity ($P = 7.1^{E-4}$). Analysis of mRNA levels confirmed reduced expression of Tyr and Dct, two pigmentation genes in both Pten WT and mutant melanoma cells derived from the PDK1 KD tumors (Fig S6). Likewise, lack of PDK1 in these melanomas also attenuated the expression of epithelial mesenchymal transition (EMT)-related genes (28), ZEB1 and MMP3 (Fig. S6). Analysis of three melanoma lines revealed slight differences (i.e., effect on Tyr level in YUMM1.9 and on MMP3 in YUMM1.5 cells was limited, compared with changes seen in the other two cultures), pointing to heterogeneity among the cell types used here. These findings points to a number of genes that could be further explored as markers for the stratification of melanoma patients for therapy by PDK1 inhibition.

DISCUSSION

A number of pathways are known to contribute to melanoma development and progression, including the MAPK signaling pathway, which is deregulated in more than 70% of melanomas (*NRAS* and *BRAF* mutations), and the PI3K/AKT signaling pathway, which is deregulated in more than 50% of these tumors, in part due to genetic mutations and in part due to altered post translational modifications (29,30). Using genetic and pharmacological inhibitors, we have previously demonstrated the importance of the master AGC kinase - PDK1 - for the development and metastasis of $BRAF^{V600E}$ $PTEN^{-/-}$ melanomas (5). Here, we extend those findings to show that PDK1 also plays an important role in melanomas harboring WT *PTEN*, which includes about 70% of human melanomas. Significantly, we found that PDK1 actually plays a more pronounced role in *PTEN* WT than *PTEN* mutant genotypes, a finding that is expected due to the preserved PTEN activity, which harnesses AKT and related PI3K components. Together, our findings further our appreciation for the impact of PDK1 to the AGC kinase landscape.

The significance of our observations is highlighted in synthetic lethal screens by the identification of pan PI3K inhibitor that effectively synergize with PDK1i, particularly in PTEN WT melanomas, suggesting that the focused targeting of the PI3K/PDK1 signaling axis might represent a novel therapeutic modality for PTEN WT melanomas. A similar approach with combination MEKi and BRAFi has produced promising results in ongoing clinical trials (31). Notably, our data point to a gene signature that distinguishes between PDK1i-sensitive melanomas (which express low levels of pigmentation genes associated with MITF signaling) and PDK1i-resistant melanomas (which express inflammation-related genes, including IL-6 and IL-3); this signature could potentially be used for the stratification of patients for PDK1-targeted therapies. Given the recent finding that low MITF expression correlates with resistance of melanomas to BRAFi (32), it would be of interest to further

Author Manuscript Author Manuscript Author Manuscript Author Manuscript

examine the possibility that targeting the PDK1 pathway might also be efficient for inhibiting the resistance phenotype. Notably, PDK1 deficient melanomas also exhibited reduced ZEB1 and MMP3 expression, pointing to PDK1 role in control of the EMT, explaining the reduced metastasis observed in vivo and attenuated growth in 3D in culture. Of interest, our results reveal that inhibition of either PDK1 or SGK3 decreased the phosphorylation of 4-EBP1, pointing to possible role of these AGC kinases in the regulation of CAP-dependent translation. Consistent with these observations, eIF4F, another component of this translation initiation complex, was recently linked with the resistance to anti-BRAF and anti-MEK therapies in BRAF mutant melanoma, colon and thyroid cancer cells (33).

PDK1 inhibitors that are suitable for use in clinical trials have not yet been developed. Although the PDK1i used in our study (GSK2334470) is quite specific and exhibits excellent properties for work with cultured cells (22,34), it is unsuitable for further preclinical or clinical development. Other PDK1 inhibitors are currently being developed, which might exhibit acceptable safety profiles and be eligible for further advanced clinical evaluation.

An alternative approach to inhibiting PDK1 is to identify and target one or more downstream PDK1 substrates that are crucial for melanoma development and progression. In this regard, we report here that the genetic and pharmacological inhibition of SGK3 largely phenocopies the effects of PDK1 inhibition on melanoma cells, including growth arrest in G1 phase. Our findings are consistent with earlier reports that pointed to the role of SGK3 in melanoma (8).

The repertoire of potential targets for melanoma therapy is expanding considerably, thanks in large part to the extensive knowledge gained from mechanistic and clinical studies. As a result, future clinical management options will be more extensive and are likely to include modulators of pathways that are independent of the MAPK signaling axis. Our data substantiate the importance of PDK1 and one of its downstream substrates, SGK3, for melanoma development and progression and further suggest that inhibitors of this signaling pathway might be useful for the development of clinical management options for melanoma.

Supplementary Material

Refer to Web version on PubMed Central for supplementary material.

Acknowledgments

We thank Yale SPORE in Skin Cancer and TGEN for cell lines used in the present study. We thank Dario Alessi for providing the conditional *Pdk1*$^{-/-}$ mice and Vince Hearing for the kind gift of the Tyrp1 antibodies. We also thank members of the Ronai lab for extensive discussions. ZAR gratefully acknowledges support from the NCI (CA179170 and CA128814), the Hervey Family Non-endowment Fund at The San Diego Foundation, and the Melanoma Research Foundation.

References

1. Hodis E, Watson IR, Kryukov GV, Arold ST, Imielinski M, Theurillat JP, et al. A landscape of driver mutations in melanoma. Cell. 2012; 150(2):251–63. [PubMed: 22817889]

Author Manuscript Author Manuscript Author Manuscript Author Manuscript

2. Mora A, Komander D, van Aalten DM, Alessi DR. PDK1, the master regulator of AGC kinase signal transduction. Seminars in cell & developmental biology. 2004; 15(2):161–70. [PubMed: 15209375]

3. Pearce LR, Komander D, Alessi DR. The nuts and bolts of AGC protein kinases. Nature reviews Molecular cell biology. 2010; 11(1):9–22.

4. Rintelen F, Stocker H, Thomas G, Hafen E. PDK1 regulates growth through Akt and S6K in Drosophila. Proceedings of the National Academy of Sciences of the United States of America. 2001; 98(26):15020–5. [PubMed: 11752451]

5. Scortegagna M, Ruller C, Feng Y, Lazova R, Kluger H, Li JL, et al. Genetic inactivation or pharmacological inhibition of Pdk1 delays development and inhibits metastasis of Braf(V600E)::Pten(−/−) melanoma. Oncogene. 2014; 33(34):4330–9. [PubMed: 24037523]

6. Davies MA, Stemke-Hale K, Lin E, Tellez C, Deng W, Gopal YN, et al. Integrated Molecular and Clinical Analysis of AKT Activation in Metastatic Melanoma. Clinical cancer research : an official journal of the American Association for Cancer Research. 2009; 15(24):7538–46. [PubMed: 19996208]

7. Zhou XP, Gimm O, Hampel H, Niemann T, Walker MJ, Eng C. Epigenetic PTEN silencing in malignant melanomas without PTEN mutation. The American journal of pathology. 2000; 157(4): 1123–8. [PubMed: 11021816]

8. Vasudevan KM, Barbie DA, Davies MA, Rabinovsky R, McNear CJ, Kim JJ, et al. AKT-independent signaling downstream of oncogenic PIK3CA mutations in human cancer. Cancer cell. 2009; 16(1):21–32. [PubMed: 19573809]

9. Sato S, Fujita N, Tsuruo T. Involvement of 3-phosphoinositide-dependent protein kinase-1 in the MEK/MAPK signal transduction pathway. The Journal of biological chemistry. 2004; 279(32): 33759–67. [PubMed: 15175348]

10. Zeng X, Xu H, Glazer RI. Transformation of mammary epithelial cells by 3-phosphoinositide-dependent protein kinase-1 (PDK1) is associated with the induction of protein kinase Calpha. Cancer research. 2002; 62(12):3538–43. [PubMed: 12068001]

11. Gagliardi PA, di Blasio L, Orso F, Seano G, Sessa R, Taverna D, et al. 3-phosphoinositide-dependent kinase 1 controls breast tumor growth in a kinase-dependent but Akt-independent manner. Neoplasia. 2012; 14(8):719–31. [PubMed: 22952425]

12. Bruhn MA, Pearson RB, Hannan RD, Sheppard KE. Second AKT: the rise of SGK in cancer signalling. Growth Factors. 2010; 28(6):394–408. [PubMed: 20919962]

13. Tessier M, Woodgett JR. Serum and glucocorticoid-regulated protein kinases: variations on a theme. Journal of cellular biochemistry. 2006; 98(6):1391–407. [PubMed: 16619268]

14. Xu J, Wan M, He Q, Bassett RL Jr, Fu X, Chen AC, et al. SGK3 is associated with estrogen receptor expression in breast cancer. Breast cancer research and treatment. 2012; 134(2):531–41. [PubMed: 22576469]

15. Sommer EM, Dry H, Cross D, Guichard S, Davies BR, Alessi DR. Elevated SGK1 predicts resistance of breast cancer cells to Akt inhibitors. The Biochemical journal. 2013; 452(3):499–508. [PubMed: 23581296]

16. Tworkoski K, Singhal G, Szpakowski S, Zito CI, Bacchiocchi A, Muthusamy V, et al. Phosphoproteomic screen identifies potential therapeutic targets in melanoma. Molecular cancer research : MCR. 2011; 9(6):801–12. [PubMed: 21521745]

17. Dankort D, Curley DP, Cartlidge RA, Nelson B, Karnezis AN, Damsky WE Jr, et al. Braf(V600E) cooperates with Pten loss to induce metastatic melanoma. Nature genetics. 2009; 41(5):544–52. [PubMed: 19282848]

18. Lawlor MA, Mora A, Ashby PR, Williams MR, Murray-Tait V, Malone L, et al. Essential role of PDK1 in regulating cell size and development in mice. The EMBO journal. 2002; 21(14):3728–38. [PubMed: 12110585]

19. Tibes R, Qiu Y, Lu Y, Hennessy B, Andreeff M, Mills GB, et al. Reverse phase protein array: validation of a novel proteomic technology and utility for analysis of primary leukemia specimens and hematopoietic stem cells. Molecular cancer therapeutics. 2006; 5(10):2512–21. [PubMed: 17041095]

Author Manuscript Author Manuscript Author Manuscript Author Manuscript

20. Wang Y, Zhou D, Chen S. SGK3 is an androgen-inducible kinase promoting prostate cancer cell proliferation through activation of p70 S6 kinase and up-regulation of cyclin D1. Mol Endocrinol. 2014; 28(6):935–48. [PubMed: 24739041]
21. Sherk AB, Frigo DE, Schnackenberg CG, Bray JD, Laping NJ, Trizna W, et al. Development of a small-molecule serum- and glucocorticoid-regulated kinase-1 antagonist and its evaluation as a prostate cancer therapeutic. Cancer research. 2008; 68(18):7475–83. [PubMed: 18794135]
22. Najafov A, Sommer EM, Axten JM, Deyoung MP, Alessi DR. Characterization of GSK2334470, a novel and highly specific inhibitor of PDK1. The Biochemical journal. 2011; 433(2):357–69. [PubMed: 21087210]
23. Yang TM, Barbone D, Fennell DA, Broaddus VC. Bcl-2 family proteins contribute to apoptotic resistance in lung cancer multicellular spheroids. American journal of respiratory cell and molecular biology. 2009; 41(1):14–23. [PubMed: 19097992]
24. Barbone D, Ryan JA, Kolhatkar N, Chacko AD, Jablons DM, Sugarbaker DJ, et al. The Bcl-2 repertoire of mesothelioma spheroids underlies acquired apoptotic multicellular resistance. Cell death & disease. 2011; 2:e174. [PubMed: 21697949]
25. Burger MT, Pecchi S, Wagman A, Ni ZJ, Knapp M, Hendrickson T, et al. Identification of NVP-BKM120 as a Potent, Selective, Orally Bioavailable Class I PI3 Kinase Inhibitor for Treating Cancer. ACS medicinal chemistry letters. 2011; 2(10):774–9. [PubMed: 24900266]
26. Aziz SA, Jilaveanu LB, Zito C, Camp RL, Rimm DL, Conrad P, et al. Vertical targeting of the phosphatidylinositol-3 kinase pathway as a strategy for treating melanoma. Clinical cancer research : an official journal of the American Association for Cancer Research. 2010; 16(24): 6029–39. [PubMed: 21169255]
27. Park ES, Rabinovsky R, Carey M, Hennessy BT, Agarwal R, Liu W, et al. Integrative analysis of proteomic signatures, mutations, and drug responsiveness in the NCI 60 cancer cell line set. Molecular cancer therapeutics. 2010; 9(2):257–67. [PubMed: 20124458]
28. Caramel J, Papadogeorgakis E, Hill L, Browne GJ, Richard G, Wierinckx A, et al. A switch in the expression of embryonic EMT-inducers drives the development of malignant melanoma. Cancer cell. 2013; 24(4):466–80. [PubMed: 24075834]
29. Parsons R. Human cancer, PTEN and the PI-3 kinase pathway. Seminars in cell & developmental biology. 2004; 15(2):171–6. [PubMed: 15209376]
30. Correia NC, Girio A, Antunes I, Martins LR, Barata JT. The multiple layers of non-genetic regulation of PTEN tumour suppressor activity. Eur J Cancer. 2014; 50(1):216–25. [PubMed: 24054978]
31. Abdel-Wahab O, Klimek VM, Gaskell AA, Viale A, Cheng D, Kim E, et al. Efficacy of intermittent combined RAF and MEK inhibition in a patient with concurrent BRAF- and NRAS-mutant malignancies. Cancer discovery. 2014; 4(5):538–45. [PubMed: 24589925]
32. Van Allen EM, Mouw KW, Kim P, Iyer G, Wagle N, Al-Ahmadie H, et al. Somatic ERCC2 mutations correlate with cisplatin sensitivity in muscle-invasive urothelial carcinoma. Cancer discovery. 2014
33. Boussemart L, Malka-Mahieu H, Girault I, Allard D, Hemmingsson O, Tomasic G, et al. eIF4F is a nexus of resistance to anti-BRAF and anti-MEK cancer therapies. Nature. 2014; 513(7516):105–9. [PubMed: 25079330]
34. Najafov A, Shpiro N, Alessi DR. Akt is efficiently activated by PIF-pocket- and PtdIns(3,4,5)P3-dependent mechanisms leading to resistance to PDK1 inhibitors. The Biochemical journal. 2012; 448(2):285–95. [PubMed: 23030823]

Author Manuscript Author Manuscript Author Manuscript Author Manuscript

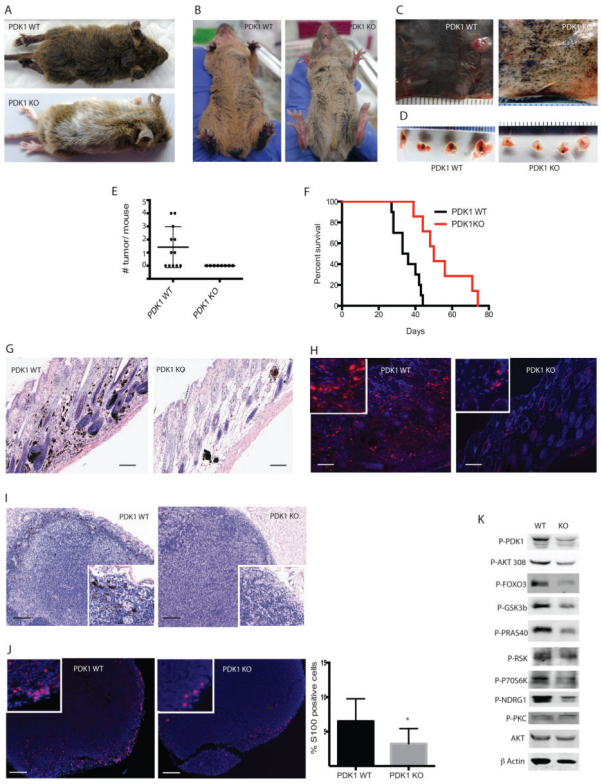

Figure 1. Loss of PDK1 inhibits the onset of melanoma development and delays metastasis

(**A**–**B**) Representative images of PDK1 WT (*Braf*^{V600E}*::Cdkn2a*$^{-/-}$*::Pten*$^{+/+}$*::Pdk1*$^{+/+}$) or PDK1 KO (*Braf*^{V600E}*::Cdkn2a*$^{-/-}$*::Pten*$^{+/+}$*::Pdk1*$^{-/-}$) mice 21 days after administration of 4-HT. (**C**–**D**) Representative images of the dorsal skin (**C**) and lymph nodes (**D**) from PDK1 WT and PDK1 KO mice 38 days after systemic administration of 4-HT. (**E**) Quantification of tumors in PDK1 WT and PDK1 KO mice (N = 12 and 8, respectively). (**F**) Kaplan-Meier survival curves of PDK1 WT and PDK1 KO mice (N = 16 and 18, respectively). $P < 0.001$ by log-rank (Mantel-Cox) test. (**G**–**H**) H&E stained (**G**) and S100 immunostained (**H**) skin sections from PDK1 WT and PDK1 KO mice 38 days after 4-HT administration. Bars = 100 μm. (**I**–**J**) H&E stained (**I**) and S100 (**J**) immunostained lymph nodes from PDK1 WT and PDK1 KO mice 38 days after administration of 4-HT. Bars = 100 μm. Graph shows mean ± SEM of S100+ cells from 3 animals per genotype. *$P < 0.005$. (**K**) Western blot analysis of the indicated proteins in primary melanoma cultures derived from PDK1 WT and PDK1 KO mice.

Author Manuscript Author Manuscript Author Manuscript Author Manuscript

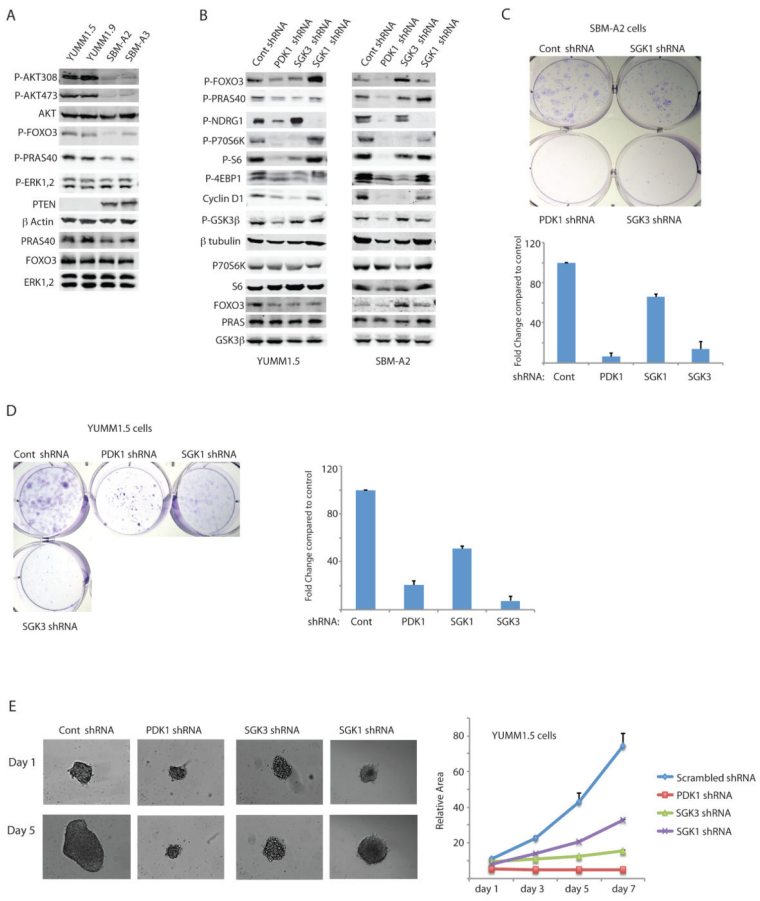

Figure 2. shRNA-mediated inhibition of PDK1 or SGK3 suppresses phosphorylation of target proteins, expression of cyclin D1, and growth of melanoma cells

(A) Western blot analysis of the indicated proteins in primary melanoma cultures derived from *Braf*^{V600E}*::Cdkn2a*$^{-/-}$*::PTEN*$^{-/-}$ mice (YUMM1.5 and YUMM1.9) or *Braf*^{V600E}*::Cdkn2a*$^{-/-}$*::PTEN*$^{+/+}$ mice (SBM-A2 and SBM-A3). (**B**) Western blot analysis of the indicated proteins from YUMM1.5 and SBM-A2 melanoma cells expressing control, *Sgk1*-, *Pdk1*-, or *Sgk3*-targeted shRNA. (**C–D**) Colony formation assay of SBM-A2 (**C**) and YUMM1.5 (**D**) cultures expressing the indicated shRNAs. Individual wells shown are representative of three experiments with triplicate cultures. The graph represents the quantification of colony forming ability compared to control shRNA. Error bars represent SEM. (**E**) Representative images of YUMM1.5 spheroids expressing the indicated shRNAs. Relative spheroid sizes were quantified using ImageJ software (NIH) and are presented as the mean ± SEM of ≥6 spheroids per group.

Author Manuscript
Author Manuscript
Author Manuscript
Author Manuscript

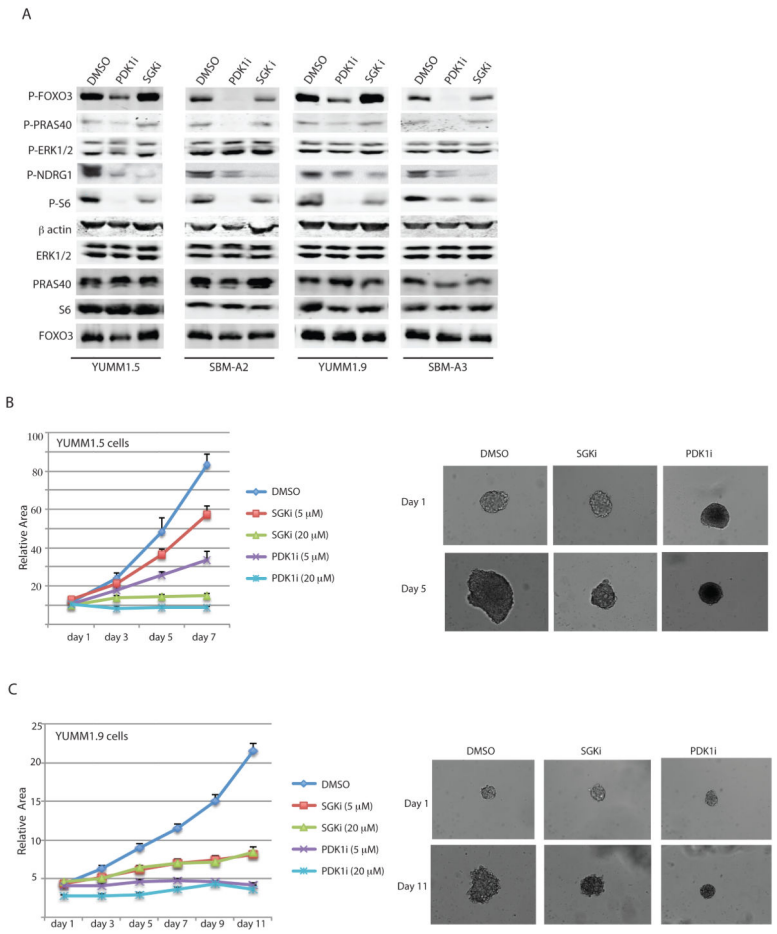

Figure 3. Pharmacological inhibition of PDK1 or SGK3 inhibits target protein phosphorylation and melanoma cell growth

(**A**) Western blot analysis of the indicated proteins in YUMM1.5, YUMM1.9, SBM-A2, and SBM-A3 cells treated for 24 h with DMSO (vehicle), 10 μM GSK2334470 (PDK1i), or 10 μM GSK650394 (SGKi). (**B–C**) Spheroid formation by YUMM1.5 (**B**) and YUMM1.9 (**C**) cells incubated with 5 or 20 μM inhibitors. Spheroid volumes were quantified on the indicated days as described for Figure 2. Results are the mean ± SEM of ≥6 spheroids per group.

Author Manuscript Author Manuscript Author Manuscript Author Manuscript

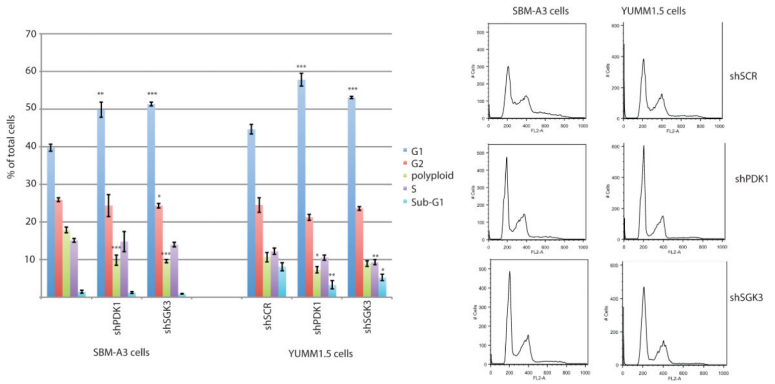

Figure 4. Inhibition of PDK1 or SGK3 induces cell cycle arrest in G1

Cell cycle distribution of SBM-A3 and YUMM1.5 cells stably expressing control shRNA (shSCR) or *Pdk1*- or *Sgk3*-targeted shRNAs. **Left**: Percentage of cells in the indicated cell cycle phases. Values are the mean ± SEM of biological triplicates. **Right**: Representative FACS profiles of the DNA content (propidium iodide staining) of cells expressing the indicated shRNAs. targeted*$P < 0.05$, **$P < 0.001$, ***$P < 0.0001$.

Author Manuscript Author Manuscript Author Manuscript Author Manuscript

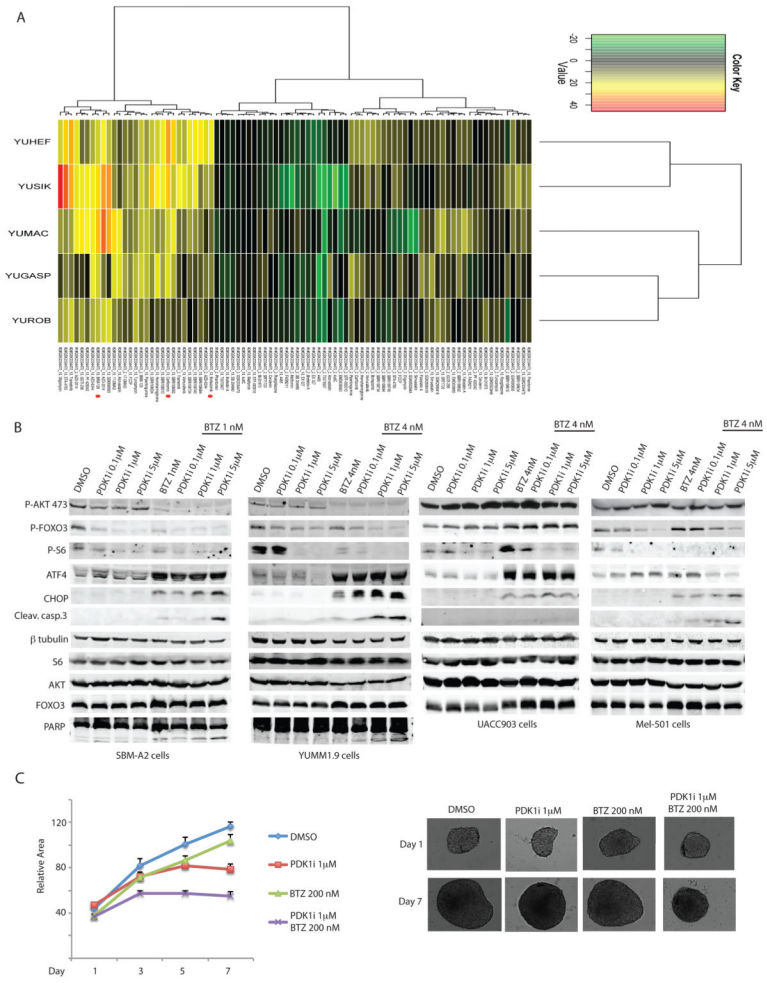

Figure 5. Combination screen of PDK1i against 45 candidate test agents

(**A**) Heat map of model-free area under the curve (AUC) of GSK2334470 at each of the two concentrations tested with unsupervised clustering of test agents (rows) and cell lines (columns). Red dots mark Bortezomib, Carfilzomib, and BKM-120 combinations with 10 μM GSK2334470. Dilutions of test agents were combined with either 0.1% DMSO vehicle, 2 μM GSK2334470, or 10 μM GSK2334470 and incubated with cell lines and assayed after 3 days with CellTiterGlo as described in Methods. Cell lines tested were YUROB, YUHEF (WT *BRAF*,*NRAS*), YUMAC, YUSIK (BRAF), YUGASP (*NRAS*). (**B**) Western blot analysis of the indicated proteins in mouse melanoma cells SBM-A2 and YUMM1.9, and human melanoma cell lines UACC903 and Mel501 treated for 24 h with 0.1, 1, or 5 μM of GSK2334470 (PDK1i) in the presence or absence of the proteasome inhibitor bortezomib (BTZ) at 1 nM (SBM-A2) or 4 nM (YUMM1.9, UACC903, Mel501). (**C**) Growth of YUMM1.5 spheroids treated with the indicated concentrations of GSK2334470 (PDK1i) and BTZ alone or in combination. Relative areas were calculated as described for Figure 2. Values are the mean ± SEM of ≥6 spheroids per group.

Author Manuscript Author Manuscript Author Manuscript Author Manuscript

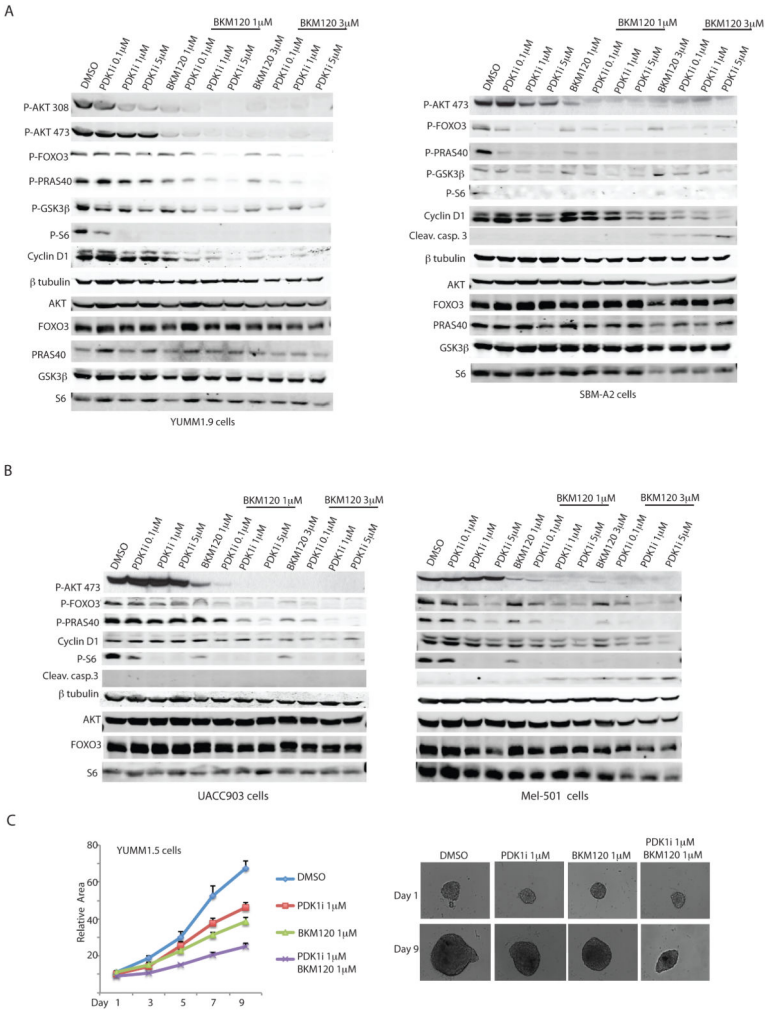

Figure 6. PDK1 and PI3K/mTOR inhibitors synergize to suppress melanoma cell growth

(**A**) Western blot analysis of the indicated proteins in YUMM1.9 and SBM-A2 cells treated for 24 h with 0.1, 1, or 5 μM of GSK2334470 (PDK1i) in the presence or absence of 1 or 3 μM of the dual PI3K/mTOR inhibitor BKM120. (**B**) Western blot analysis of the indicated proteins in the human melanoma cell lines UACC903 and Mel501 treated with 0.1, 1, or 5 μM of GSK2334470 (PDK1i) in the presence or absence of 1 or 3 μM of BKM120. (**C**) Growth of YUMM1.5 spheroids treated with the indicated concentrations of GSK2334470 (PDK1i) and BKM120 alone or in combination. Relative areas were calculated as described for Figure 2. Values are the mean ± SEM of ≥6 spheroids per group.

Author Manuscript
Author Manuscript
Author Manuscript
Author Manuscript

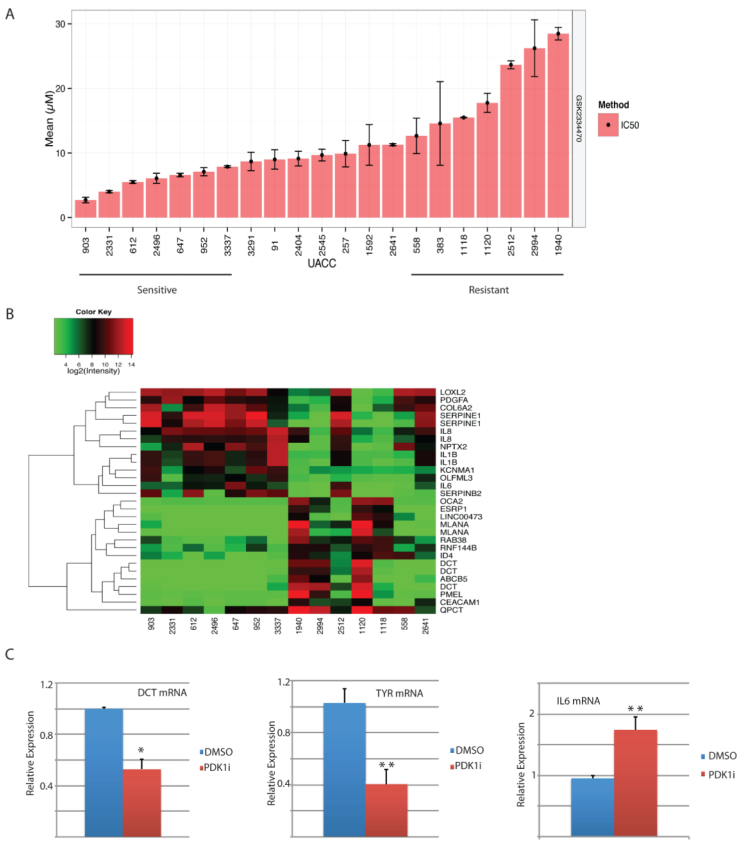

Figure 7. Stratification of human melanomas by sensitivity to PDK1 inhibition

(**A**) The mean IC50 for GSK2334470 inhibition of growth of 19 human melanoma cell lines was used to segregate cell lines into sensitivity or resistance to the inhibitor. (**B**) Heat map of the results of the IPA analysis showing the genes/pathways most significantly altered ($P < 0.05$; fold change >1.5) by GSK2334470 (1178 differentially expressed genes). (**C**) qPCR analysis of *Dct*, *Tyr*, and *Il6* mRNA in YUMM1.5 cells treated with DMSO or GSK2334470 at 5 μM for 24 h (*Dct* and *Tyr*) or at 10 μM for 6 h (*Il6*). Values are the mean ± SEM of biological triplicates. $*P < 0.05$, $**P < 0.01$.